Materials International
Open-Access Journal (ISSN: 2668-5728)

Review
Volume 8, Issue 1, 2026, 2
https://doi.org/10.33263/Materials81.002

Towards Smarter Composites: Carbon-Based Sensors for Structural Health Monitoring

Thaís Larissa do Amaral Montanheiro [1,*], Evelyn Alves Nunes Simonetti [2], Iriana Garcia Guerra [3], Alexander Hiroshi Kasama [4], Jandro Lario Abot [3], Domingos Alves Rade [1]

[1] Technological Institute of Aeronautics, Division of Mechanical Engineering, São José dos Campos, SP, Brazil; thais@ita.br (T.L.A.M.); rade@ita.br (D.A.R.);
[2] Department of Chemistry, Federal Institute of Education, Science and Technology of São Paulo (IFSP), São José dos Campos, SP, Brazil; evelyn@ifsp.edu.br;
[3] Department of Mechanical Engineering, The Catholic University of America, Washington, DC, United States of America; garciaguerra@cua.edu (I.G.G.); abot@cua.edu (J.L.A.);
[4] CENPES, Petrobras, Rio de Janeiro, RJ, Brazil; kasama@petrobras.com.br;
* Correspondence: thais@ita.br;

Received: 14.08.2025; Accepted: 15.11.2025; Published: 10.03.2026

Abstract: Structural Health Monitoring (SHM) technologies are essential for ensuring the safety, integrity, and reliability of critical infrastructures. Carbon-based nanomaterials, including carbon nanotubes (CNTs),, carbon nanotube yarns (CNTYs), and graphene, have emerged as highly promising sensing materials due to their remarkable electrical conductivity, flexibility, and mechanical performance. This review summarizes the most recent advances in CNT-, CNTY-, and graphene-based sensors developed for SHM applications, with emphasis on their fabrication methods, sensing mechanisms, and performance metrics. The comparative analysis highlights how these materials enable accurate strain and damage detection in composite structures, thereby providing pathways toward multifunctional, lightweight sensing systems. Finally, the main challenges and future prospects of carbon-based SHM sensors are discussed, including large-scale manufacturing, stability under cyclic loading, and integration with data-driven diagnostic tools for next-generation intelligent structures.

Keywords: Structural health monitoring; *in-situ* sensing; carbon nanotube; carbon nanotube yarn; graphene.

1. Introduction

Due to their unique properties, carbon-based materials have seen significant advancements and an increasing range of applications in recent years. Carbon-based materials such as graphene and carbon nanotubes (CNTs) have significantly impacted the energy storage and conversion industry, becoming essential for applications in portable electronics and electric vehicles. Carbon-based compounds enhance the stability and conductivity of battery electrodes, increasing capacity and prolonging lifespan. Additionally, these compounds improve the durability and efficiency of fuel cells by serving as catalysts and support materials. Carbon-based materials, such as graphene oxide, can also be used in water filtration systems to remove contaminants and pathogens. Composite materials, which combine the best features of their constituent elements, offer superior properties that have made them indispensable in

engineering applications. Compared to traditional materials, composites provide enhanced strength, durability, manufacturability, and versatility. Typically, they consist of a reinforcement phase and a matrix. These materials are used in a variety of industries, including automotive, aerospace, and construction [1–4].

Structural Health Monitoring (SHM) is a comprehensive approach for assessing the integrity of structures. SHM addresses issues arising from material degradation due to environmental factors and service loads (e.g., fatigue and corrosion), as well as unexpected external events such as earthquakes and impacts. Major structural failures can lead to severe economic consequences and loss of life, making SHM a crucial tool in modern engineering. Non-Destructive Inspection (NDI) methods within SHM have seen significant advancements over time. The capabilities of NDI have been enhanced through improvements in experimental techniques, hardware upgrades, statistical methods, analytical simulations, and signal processing [5–7].

The primary objectives of SHM systems are to optimize structural usage, reduce downtime, and prevent catastrophic failures. Performance-based inspections aim to replace scheduled and periodic maintenance in SHM systems, reducing human error and labor costs while enhancing reliability. For example, SHM is critical for wind turbine blades, as blade failures are among the leading causes of turbine downtime. Leading-edge erosion, lightning strikes, ice accumulation, and fatigue are the main sources of blade damage, all of which can be monitored and managed through SHM. An SHM system integrates sensors either embedded within or mounted on the surface of the structure, functioning like a nervous system to detect faults and damage. Various Non-Destructive Testing (NDT) techniques and tools are utilized in SHM, including metallic foil strain gauges, fiber Bragg grating (FBG) optical fiber sensors, accelerometers, X-rays, ultrasonic monitoring, infrared thermal imaging, piezoelectric ceramic sensors, and acoustic emission (AE) technology [6,7].

Despite these advancements and the potential benefits, SHM systems are not yet widely adopted due to challenges such as cost and the need for nearly zero false-alarm rates. However, the potential benefits of SHM are considerable, including minimizing service interruptions and extending the lifespan of structural systems [5].

This paper reviews the recent advancements in the use of carbon-based materials as sensors for structural health monitoring in composites, with a focus on the past four years. Specifically, it discusses carbon nanotubes, carbon nanotube yarns (or fibers), and graphene.

1.1. Review methodology.

This review was conducted using the Scopus, Web of Science, and ScienceDirect databases. The search covered the last five years, using the keywords “carbon nanotube sensor”, “CNT yarn”, “graphene sensor”, and “structural health monitoring”. Only peer-reviewed journal articles and review papers written in English were included. Conference abstracts and non-indexed reports were excluded. The focus was on studies reporting quantitative parameters, such as gauge factor, sensitivity, operating range, and real-time monitoring capabilities, for carbon-based SHM sensors.

2. Carbon-based materials as sensors for SHM

2.1. Carbon nanotubes.

Carbon nanotubes are allotropes of carbon with sp^2 hybridization, similar to graphene [8,9]. This type of hybridization creates a layered structure with strong in-plane bonds and weak out-of-plane van der Waals interactions, allowing graphite sheets to slide along their planes [10]. CNTs are formed by concentrically rolled graphene sheets, with nanometric diameters, and can be either single (Single-Walled Carbon Nanotubes – SWCNTs) or multi-walled (Multi-Walled Carbon Nanotubes – MWCNTs) (Figure 1) [10–12]. CNTs exhibit armchair, zigzag, and chiral configurations, which depend on the angle at which the graphite sheet rolls up [13,14]. The electronic properties of CNTs are strongly influenced by their chirality, with some CNTs exhibiting metallic or semiconductor behavior [15].

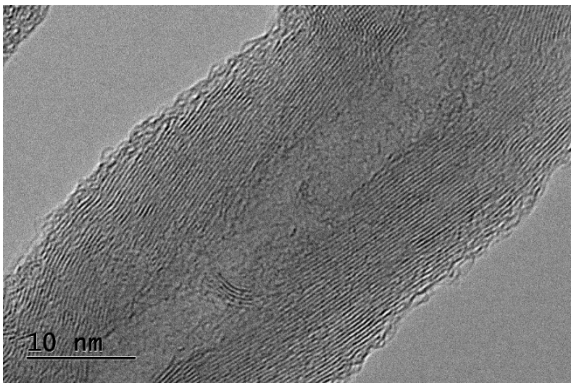

Figure 1. Transmission electron microscopy (TEM) image of multi-walled carbon nanotubes (MWCNTs).

The most common techniques for producing CNTs are chemical vapor deposition (CVD), a low-temperature method, laser ablation, and arc discharge [13,16,17]. Numerous studies have documented the outstanding mechanical and physical properties of CNTs, including high fracture toughness, high elastic modulus, and remarkable resistance to bending and rupture [18,19].

Owing to their exceptional mechanical, electrical, thermal, and chemical properties, CNTs are used in semiconductors and electronics for fabricating high-performance integrated circuit interconnects and transistors. CNTs also improve the electrical conductivity of polymers for electromagnetic interference (EMI) shielding and antistatic materials. Furthermore, CNTs enhance mechanical strength, stiffness, and toughness, making them valuable in the aerospace, automotive, and construction industries [20–22]. In energy storage and conversion, CNTs are used to improve fuel cell durability and efficiency, increase supercapacitor energy density, and enhance lithium-ion battery performance [23,24]. Their high thermal conductivity is advantageous for heat dissipation in electronic devices and thermal management applications, while their sensitivity makes them suitable for chemical and biological sensors [25]. In medicine, CNTs are used as contrast agents in imaging procedures, as well as carriers for targeted drug delivery and photothermal cancer therapy [26]. Additionally, CNTs are utilized in environmental applications, such as air and water filtration, due to their high adsorption capacity. CNTs are also integrated into textiles to create smart materials with enhanced mechanical properties, environmental sensing capabilities, and electrical conductivity. Finally, CNTs are used in optoelectronics for flexible, transparent displays, light-emitting devices, and photodetectors, highlighting their versatility across advanced technologies.

Piezoresistivity, the ability of a material to change its electrical resistance in response to mechanical strain, is a key property of CNTs. This property arises from the sp^2-hybridized carbon atoms in the rolled-up graphene sheets. When CNTs are mechanically bent, compressed, or stretched, their electrical band structure and density of states near the Fermi level are altered, leading to changes in their electrical conductivity [27].

CNTs exhibit remarkable strain sensitivity due to their one-dimensional (1D) structure and quantum confinement effects. Even small mechanical deformations can cause significant changes in electrical resistance, making CNT-based sensors highly sensitive and capable of detecting even minute strain variations. The piezoresistive properties of CNTs can be tuned by adjusting factors such as their diameter, chirality, and the type of mechanical strain applied. Both SWCNTs and MWCNTs display piezoresistivity, but SWCNTs generally offer higher sensitivity due to their simpler structure [28].

CNT-based sensors have a high gauge factor, making them highly sensitive to strain and enabling precise stress and strain measurements across various environments. The exceptional strength, flexibility, and chemical stability of CNTs also ensure the reliability and longevity of these sensors. Ongoing research and development are expected to further the integration of piezoresistive CNTs into functional devices, providing innovative solutions for advanced sensing technologies.

Al-Bahrani *et al*. [29] investigated self-sensing nanocomposites designed to predict structural damage. Nanocomposites containing 0–4 wt% multi-walled carbon nanotubes (MWCNTs) were produced using a phenolic matrix. The study identified a percolation threshold between 0 and 0.5 wt% MWCNT, indicating uniform nanotube dispersion within the polymer, with agglomeration observed above 2.0 wt%. An increase in MWCNT content reduced indentation displacement and matrix plasticity, revealing a transition to elastic–plastic behavior associated with the formation of conductive pathways. Electrical resistance changes ($\Delta R/R_0$) correlated with applied load and damage progression, demonstrating the material's sensitivity to micro-scale strain. The highest piezoresistive response occurred at 0.5 wt% MWCNT, where the conductive network was most effective in detecting cumulative damage. The authors concluded that nanocomposites near the percolation threshold exhibit enhanced mechanical loading responsiveness, supporting their potential as self-sensing materials for damage monitoring.

Duan *et al*. [30] developed a methyl cellulose-based CNT ink for strain and pressure sensors containing 2 wt% CNT. The ink was printed onto flexible substrates to fabricate textile strain sensors and sponge-based pressure sensors, both of which were encapsulated in PDMS. Transmission electron microscopy (TEM) and UV–Vis spectroscopy confirmed uniform CNT dispersion and high electrical conductivity (2.89 S/cm). The strain sensors exhibited high gauge factors (≈10 at 30% strain), outperforming conventional counterparts, and maintained stable, repeatable responses over 300 loading cycles without hysteresis. These sensors demonstrated the ability to detect both small physiological signals, such as throat vibrations, and larger joint movements, highlighting their versatility for wearable monitoring. Similarly, the sponge-based pressure sensors showed consistent piezoresistive responses under repeated compression, with performance influenced by sponge porosity and density. Overall, the CNT ink enabled lightweight, sensitive, and durable sensors suitable for applications in wearable electronics, motion tracking, and pressure detection.

Chen *et al*. [31] proposed an in-situ damage monitoring approach for glass fiber-reinforced polymers (GFRP) using a bioinspired mesh-structured piezoresistive sensor. Fiber-

reinforced composites are prone to interfacial debonding, delamination, fiber breakage, and matrix cracking, making nonintrusive defect assessment essential for structural health monitoring. The researchers designed a flexible, stretchable MWCNT/PVA mesh film inspired by spider webs, intended to be embedded within composite laminates. Compared to solid film sensors, the mesh architecture exhibited higher porosity (80–90%) and strain capacity, enhancing its flexibility and sensitivity. The gauge factor increased with strain and decreased with porosity, indicating a tunable piezoresistive response. Mechanical testing showed that GFRP composites containing the mesh sensor displayed greater elongation at break and reduced crack propagation, attributed to the sensor's ability to absorb fracture energy. In contrast, solid film sensors caused stress concentration, delamination, and reduced tensile and flexural strength. The mesh sensor also demonstrated superior stability, repeatability, and early-damage detection, closely correlating with acoustic emission data. X-ray imaging confirmed that the embedded mesh preserved the mechanical integrity of the composite while effectively tracking micro-scale damage, establishing it as a nonintrusive and reliable option for structural health monitoring.

Wang *et al*. [32] investigated MWCNT buckypapers with varying nanotube concentrations for use as multisensing elements in the structural health monitoring of glass-fiber-reinforced polymer (GFRP) composites. The buckypaper sensors were integrated onto the top and bottom surfaces of GFRP laminates and evaluated under three-point bending tests. Among the tested formulations, samples produced with 500 mg MWCNT exhibited the highest sensitivity and stability, and were therefore selected for detailed electromechanical characterization. The electrical response of the sensors correlated strongly with applied stress and strain, displaying distinct piezoresistive behaviors under tensile and compressive loading. The buckypaper positioned on the lower (tensile) surface demonstrated gauge factors significantly higher than those of commercial metallic strain gauges (GF ≈ 2.0), confirming its superior strain sensitivity. Changes in resistance followed a nonlinear trend consistent with flexural stress distribution, enabling detection of microdamage initiation and propagation. The sensors maintained stable responses under cyclic loading, indicating the durability of the conductive network. Overall, MWCNT buckypaper sensors demonstrated the ability to accurately detect and track damage in composite materials, with strong potential for integration into smart composite structures for real-time health monitoring.

2.2. Carbon nanotube yarns.

Carbon nanotube yarns (CNTYs) are continuous fibers created by twisting or braiding aligned carbon nanotubes (CNTs) (Figure 2) [33]. These yarns leverage the remarkable mechanical properties of individual CNTs, which include high tensile strength and high elastic modulus [34]. Structurally, CNTs can be classified as either single-walled (SWCNTs) with diameters between 0.4 and 2 nm, or multi-walled (MWCNTs) with diameters ranging from 2 to 100 nm [35]. This structural arrangement results in yarns that are robust, flexible, and conductive. The properties of CNTYs are profoundly influenced by the alignment and packing density of the nanotubes; highly aligned and densely packed yarns demonstrate superior characteristics, such as enhanced tensile strength and electrical conductivity, compared to yarns with lower degrees of alignment and packing density [36].

Optimal alignment angles, ideally parallel or nearly parallel to the yarn axis, improve load transfer and minimize slippage between nanotubes, thereby maximizing the yarn's

performance [37]. Furthermore, achieving high packing density reduces voids and defects, further enhancing the overall structural integrity and functional properties of CNT yarns [38].

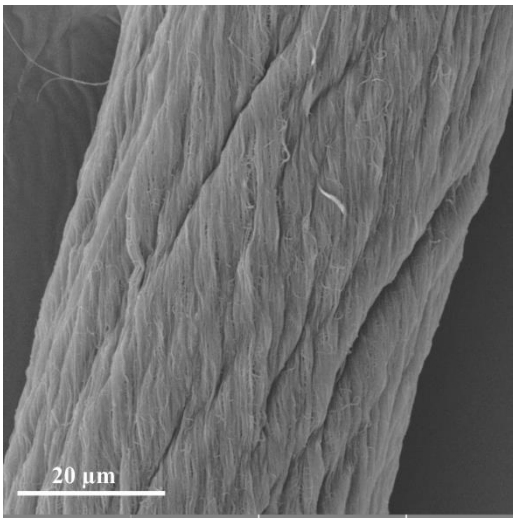

Figure 2. Scanning electron microscopy (SEM) image of CNT yarn.

CNT yarns are distinguished by their extensive potential applications due to their unique properties. They can achieve tensile strengths of several gigapascals (GPa), with values frequently ranging from 1 to 4 GPa, surpassing many conventional materials such as Kevlar and high-strength steel [39]. Additionally, CNT yarns exhibit electrical conductivities comparable to those of metals, reaching up to 10^4 S/cm, making them suitable for applications in electronics and electrical systems [40]. Their remarkable thermal conductivity facilitates efficient heat dissipation in high-performance devices [41]. Furthermore, CNT yarns are lightweight, chemically resistant, and maintain their properties under extreme conditions, including high temperatures and corrosive environments [42].

The fabrication of CNT yarns involves various sophisticated techniques, each with its distinct advantages and limitations. Common methods include spinning CNTs from liquid-crystalline solutions, dry spinning from CNT arrays, and direct synthesis via chemical vapor deposition (CVD) [43,44]. In the liquid-crystalline spinning process, CNTs are dispersed in a solution and spun into fibers as the solvent evaporates [45]. Dry spinning entails drawing CNTs from a vertically aligned array and twisting them into yarn [37]. The CVD method produces CNT yarns directly by continuously growing them on a substrate while simultaneously twisting them into fibers [46]. These techniques aim to optimize the alignment and packing density of the CNTs, thereby enhancing the mechanical and electrical properties of the yarns [47].

The integration of CNTYs into composite materials leverages their piezoresistive properties, making them effective sensors for SHM [48]. The change in electrical resistance of CNTYs under mechanical strain allows them to function as highly sensitive strain sensors [49]. This characteristic is particularly valuable in detecting deformation and damage in composite structures.

Abot *et al*. [49] made a remarkable contribution by investigating carbon nanotube yarns (CNTYs) as embedded sensors for monitoring static and dynamic responses in laminated composites. CNTYs were integrated between selected glass fiber layers during lay-up, allowing intimate contact with the matrix and enhancing strain transfer. Under quasi-static four-point bending, the CNTY sensors exhibited real-time piezoresistive responses strongly correlated with applied stress and strain, achieving gauge factors of approximately 0.33 in tension and 0.23 in compression. This sensitivity enabled the early detection of stress concentrations and

the initiation of microcracks, key to preventing structural failure. In dynamic vibration tests, CNTYs accurately captured frequency and amplitude variations under sinusoidal loading, confirming their ability to monitor both static and dynamic behaviors. Overall, the results highlight the high potential of CNTYs as multifunctional sensors for real-time structural health monitoring (SHM) in composite materials.

Building on previous research, Wang *et al*. [50] integrated CNTY sensors into braided composite structures during the weaving stage, ensuring uniform distribution and full embedding after resin infusion via VARTM. This manufacturing strategy preserved structural integrity while enabling the seamless incorporation of sensing elements. Under tensile and compressive loading, an Artificial Fish Swarm Algorithm (AFSA) was implemented to optimize the sensor network configuration in real time, improving damage localization. The piezoresistive CNTY sensors accurately detected fiber breakage and matrix cracking with sub-millimeter precision, demonstrating outstanding sensitivity and spatial resolution. These findings underscore the potential of CNTY-integrated braided composites for real-time, high-accuracy structural health monitoring (SHM) in complex and safety-critical systems.

Expanding the multifunctional potential of CNTYs, Binfaris *et al*. [51] employed them as active components in supercapacitors designed to power SHM systems. CNTYs were embedded and aligned within a polymer matrix to enhance interfacial contact with the electrolyte, significantly increasing energy storage efficiency. The resulting devices achieved energy densities of 10–20 Wh/kg and power densities up to 10,000 W/kg, values well-suited for supplying embedded SHM sensors. Beyond serving as reliable energy sources, these CNTY-based supercapacitors also contributed to the composite's mechanical reinforcement, illustrating their promise for integrated, self-powered, and durable monitoring systems in advanced structural materials.

As the final example, Uribe-Riestra *et al*. [52] developed a self-sensing glass-fiber reinforced composite by embedding CNTYs aligned longitudinally and transversely within the laminate structure. This configuration enabled distributed strain and damage detection throughout the material. The composites were evaluated under cyclic four-point bending and low-velocity impact tests that simulate operational loading conditions. Real-time monitoring of electrical resistance changes in the CNTYs revealed the initiation, accumulation, and propagation of damage, which correlated strongly with high-strain regions identified via Digital Image Correlation (DIC). The results demonstrated that integrating CNTYs enables accurate and durable in-situ structural health monitoring, with the potential to extend service life and reduce maintenance costs of composite structures.

This assessment of CNTY integration into composite materials highlights its immense potential to enhance the reliability and safety of structural components. By enabling real-time monitoring and early damage detection, CNTYs are becoming crucial for developing smart materials that maintain structural integrity under various conditions. Their dual function as sensors and reinforcements paves the way for more resilient and intelligent composites, with significant implications for aerospace, automotive, and civil engineering. As research advances, CNTYs are expected to play a central role in the future of structural health monitoring, driving safer, more efficient, and sustainable engineering solutions.

2.3. Graphene.

Graphene is a carbon allotrope consisting of a two-dimensional layer of carbon atoms arranged in a hexagonal honeycomb structure. This configuration offers exceptional properties,

including high electrical conductivity, superior mechanical strength, and excellent thermal conductivity. The sp^2 hybridization of carbon atoms in graphene results in a flat network of σ bonds, forming a rigid structure, while π bonds control interactions between different graphene layers [53].

The mechanical properties of graphene are remarkable, with an elastic modulus of approximately 1 TPa and an intrinsic strength of 130.5 GPa. These characteristics make graphene an extremely robust material, with a load-bearing capacity significantly higher than most known materials. Additionally, graphene's thermal conductivity is exceptionally high (around 5×10^3 W/mK), making it suitable for applications requiring efficient heat dissipation. The impressive mechanical properties of graphene are largely due to the sp^2 hybridization of its carbon atoms, which form strong covalent bonds in a two-dimensional plane. These bonds give graphene its incredible tensile strength and flexibility, enabling it to stretch up to 20% of its original length without breaking. These properties are particularly advantageous for applications that require robust yet lightweight materials. Similarly, the high thermal conductivity is due to ballistic phonon transport in the graphene lattice, enabling rapid heat transfer throughout the material [53–55].

Graphene oxide (GO), on the other hand, is derived from graphene through oxidation, introducing oxygen-containing functional groups into its structure. These functional groups play a critical role in modifying the material's properties, including dispersibility, chemical reactivity, and interactions with other substances [56]. Figure 3 presents a high-resolution micrograph of GO prepared by the Hummers method, highlighting its characteristic wrinkled, layered morphology. The observed structure consists of thin, transparent, overlapping nanosheets with irregular edges, typical of exfoliated GO. These sheets demonstrate significant surface area and flexibility, features that arise from the oxidation and subsequent exfoliation of graphite. The wrinkles and folds across the surface suggest the presence of oxygen-containing functional groups (such as hydroxyl, carboxyl, and epoxy groups), which disrupt the planar sp^2 carbon network and contribute to the hydrophilicity and chemical reactivity of GO. This morphology is especially advantageous for applications in nanocomposites, sensors, and filtration systems due to its enhanced interfacial interactions and mechanical reinforcement.

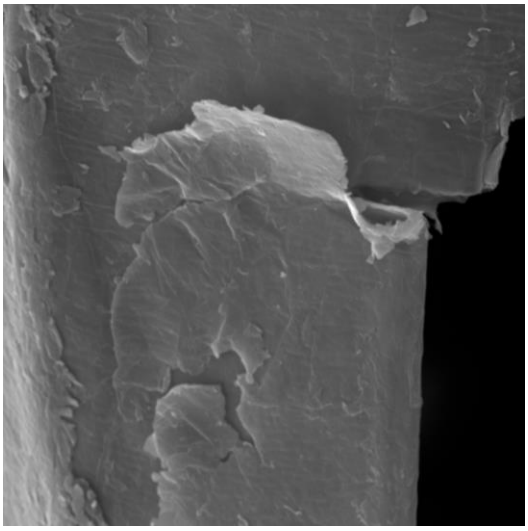

Figure 3. SEM image of graphene oxide (GO) synthesized via the modified Hummers method.

The oxygen-containing functional groups make GO highly hydrophilic, allowing it to disperse in water and other polar solvents. This property facilitates the handling of GO in solution form, enabling the fabrication of thin films, coatings, and composites through solution-

based deposition methods. Good dispersibility is essential for industrial-scale applications where uniformity and stability of suspensions are critical. In addition, the presence of oxygen-containing functional groups in GO provides multiple reactive sites for chemical modification. This reactivity allows for the functionalization of GO with various molecules, including polymers, metals, and biomolecules. GO's functionalization can be tailored to adjust its electronic, mechanical, and biological properties, making it a highly customizable material for specific applications [56,57].

In the context of SHM, graphene and GO are used as sensing elements due to their high sensitivity to structural and load variations. Graphene-based sensors can detect subtle deformations and damage in laminated composites, providing accurate, real-time information on structural integrity. Integrating these materials into SHM systems enables continuous, non-invasive monitoring, which is essential for preventive maintenance and the safety of critical structures, as shown in Figure 4 [58].

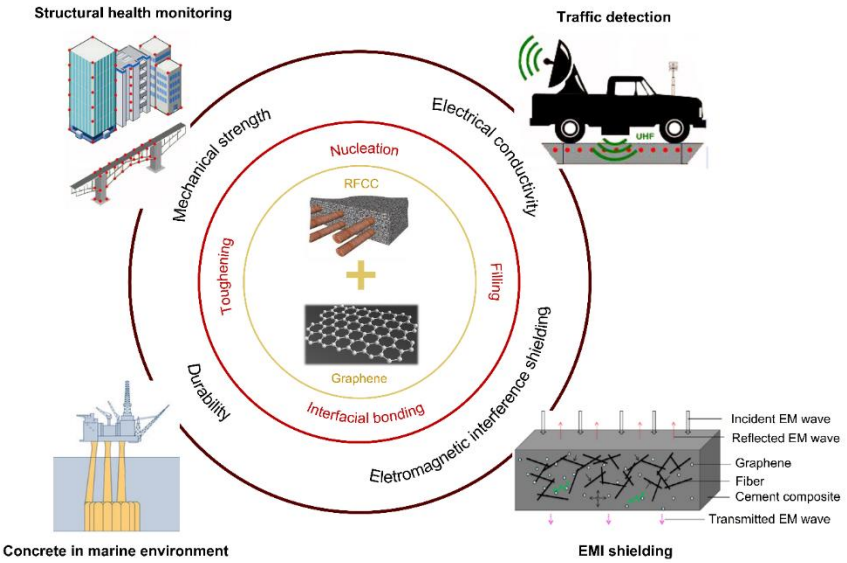

Figure 4. Schematic illustration of the multifunctional applications of graphene in SHM systems, including mechanical reinforcement, durability enhancement, electromagnetic interference (EMI) shielding, and traffic detection. Reproduced from [58], an open-access article.

The production of graphene and graphene oxide (GO) has been extensively investigated due to their exceptional properties and wide range of applications. Since the discovery of graphene in 2004 by Andre Geim and Konstantin Novoselov, several techniques have been developed to produce high-quality and large-scale graphene [59].

The first approach, known as micromechanical exfoliation or the *Scotch Tape* method, isolates graphene layers from graphite using adhesive tape [60]. Another method, electrochemical exfoliation, is a simple and high-yield process that employs graphite electrodes in aqueous or non-aqueous electrolytes, where layer separation occurs through electrode expansion under an electric field [61]. Chemical vapor deposition (CVD) represents a widely used “bottom-up” approach for large-scale production, in which carbon precursors (e.g., methane or acetylene) decompose on metal substrates such as copper or nickel under controlled temperature and pressure conditions [62].

Graphene oxide (GO) is typically obtained by oxidizing graphite to introduce oxygen-containing functional groups into its structure. The most common route is the Hummers’ method and its modifications, which use a mixture of sulfuric acid (H_2SO_4), sodium nitrate ($NaNO_3$), and potassium permanganate ($KMnO_4$)[63,64]. More recently, green synthesis

approaches have emerged, employing mild reducing agents such as ascorbic acid, plant extracts, or amino acids to minimize hazardous chemical use. These environmentally friendly methods yield high-purity GO or reduced GO (rGO), suitable for applications in biomedicine, environmental remediation, and energy storage, representing a sustainable advancement in nanomaterial production [65,66].

Structural health monitoring (SHM) aims to perform tasks such as damage detection, localization, and quantification to maintain the integrity of an entire structure. Early detection of damage is crucial to ensure proper maintenance and the reliability of structures. Graphene and its derivatives, particularly graphene oxide (GO), have emerged as promising materials for SHM due to their exceptional electrical, mechanical, and thermal properties. Several studies have demonstrated the effectiveness of graphene-based sensors in detecting various types of damage, including delamination, matrix cracking, and fiber breaking. The sensitivity and accuracy of these sensors are discussed, along with the challenges encountered, such as environmental and operational variations.

Recent advancements have demonstrated the effectiveness of embedded, non-intrusive graphene/epoxy broadband nanocomposite sensors co-cured with glass fiber-reinforced polymer (GFRP) for in situ structural health monitoring. Wang *et al*. [67] dispersed graphene nanoplatelets (GNP) in epoxy resin and combined them with the GFRP composites. The preparation involved magnetic stirring, sonication, and vacuum degassing to ensure uniform dispersion. The sensors, fabricated under various pressures, were tested for their sensing capabilities and mechanical integrity. Scanning electron microscopy (SEM) revealed uniform dispersion of GNPs and tight bonding between the sensor and the glass fibers, confirming the non-intrusive nature of the sensor. The sensor effectively captured structural responses from static strain to high-frequency ultrasonic waves up to 600 kHz, with a gauge factor of up to 26 at -25 inHg pressure, demonstrating superior sensitivity. The tensile and three-point bending tests indicated negligible intrusion of the sensor and mechanical properties comparable to those of GFRP without sensors. The sensor exhibited stable, repeatable, and reversible dynamic responses in vibration tests (300 Hz to 2 kHz) and effectively captured guided ultrasonic waves (150 kHz to 600 kHz), showing comparable performance to commercial PZT wafers. However, challenges such as ensuring uniform graphene dispersion, minimizing nanofiller agglomeration, and maintaining sensor integrity during co-curing were identified. Addressing these challenges and optimizing the fabrication process will enhance the application of graphene-based sensors in SHM of composite materials.

In a similar application, the development of thin-film graphene-based nanocomposite strain sensors has led to significant improvements in ultrasonic testing-based structural health monitoring. Guan *et al*. [68] developed a high-thermal-stability, fully spray-coated multilayer graphene/polyamide-imide (PAI) nanocomposite strain sensor capable of detecting high-frequency ultrasonic waves under unstable temperature conditions. The sensor comprised a PAI insulation/adhesion layer, a graphene/PAI sensing layer, and a silver electrode layer, all fabricated using ultrasonic atomization-assisted spray coating. The PAI matrix ensured stable electrical conductivity and strong adhesion to monitoring targets up to 160°C. SEM, thermogravimetry–differential scanning calorimetry (TG–DSC), and adhesion tests confirmed the film's morphology and thermal integrity, showing uniform graphene dispersion and high stability up to 230°C for the insulation layer and 250°C for the sensing layer. Adhesion tests demonstrated minimal degradation after ten thermal cycles, ensuring responsiveness under elevated temperatures, while electrical conductivity increased with temperature, maintaining

excellent thermal stability. For ultrasonic response evaluation, three nanocomposite sensors and four PZT wafers were mounted on an aluminum plate. The graphene/PAI sensors successfully detected both symmetric (S_0) and antisymmetric (A_0) Lamb wave modes with consistent arrival times and amplitudes. Unlike PZT sensors, whose signal amplitude decreased with temperature, the nanocomposite sensors exhibited enhanced response due to improved conductivity. The study also proposed a multi-element series design to tune sensitivity to specific wavelengths, achieving approximately 180% higher sensitivity to the A_0 mode than sensors with fewer elements. Overall, the multilayer thin-film graphene/PAI nanocomposite strain sensor demonstrated exceptional thermal stability, high sensitivity, and robust ultrasonic response, highlighting its potential for advanced SHM applications across diverse and high-temperature environments.

In another application field, such as stress and damage sensing, Gulisano *et al*. [69] investigated the incorporation of graphene nanoplatelets (GNPs) into asphalt mixtures to develop self-sensing road pavement materials. The stress- and damage-sensing responses were evaluated using digital signal processing techniques, including wavelet transform analysis of the electrical signals generated by the mixtures. The GNPs were incorporated into a Stone Mastic Asphalt (SMA 11) mixture via hand-mixing, offering a practical approach for large-scale production despite inherent challenges in achieving uniform dispersion due to strong van der Waals interactions. SEM analysis confirmed the flake-like morphology and distribution of GNPs within the asphalt binder. Volumetric and mechanical characterization showed that adding 5 wt% GNPs reduced air void content and slightly increased stiffness, though a decrease in indirect tensile strength (ITS) was observed—attributed to GNP agglomeration affecting bitumen–aggregate adhesion. The stress-sensing performance was assessed by monitoring electrical resistance under cyclic compressive loading, revealing a linear correlation between applied stress and electrical response. Higher stress levels produced increased electrical signals, while the presence of moisture enhanced ionic conduction, influencing sensitivity. For damage-sensing evaluation, digital signal processing based on wavelet transform effectively identified structural changes during loading, enabling detection of crack initiation and propagation. Both continuous and discrete wavelet analyses provided valuable insights into the piezoresistive response and structural integrity of the mixtures. Overall, the addition of 5 wt% GNPs endowed the asphalt composites with notable stress- and damage-sensing capabilities. Future studies should aim to optimize nanoparticle dispersion to improve mechanical performance and investigate long-term environmental effects, while integrating advanced digital processing and machine learning tools to enhance pavement health-monitoring applications.

For damage prediction in aircraft structural components, flexible strain sensors have emerged as crucial tools where traditional sensors are limited. Meng *et al*. [70] developed a flexible graphene/polydimethylsiloxane (GNP/PDMS) strain sensor via a mechanical coating method, combining large-area coverage, high strain capacity, and excellent sensitivity for aircraft damage detection. Graphene nanoplatelets (GNPs) were first prepared through thermal treatment and sonication, then mechanically coated onto a PDMS substrate to form a conductive composite film. SEM characterization revealed a uniform distribution of GNPs on the PDMS surface and overlapping flake structures, which established a stable conductive network essential for strain sensing. The sensors exhibited increasing resistance change rates ($\Delta R/R_0$) with applied strain, with thicker films showing higher sensitivity. Tests under strain and temperature variations demonstrated rapid response and recovery times (~0.23 s) and marked resistance increases with temperature, indicating potential for temperature sensing. In

practical tests, GNP/PDMS sensors were applied to specimens with hole-edge cracks, aircraft wing box sections, and composite structures under various loading conditions. They successfully detected crack initiation and propagation, as well as strain distribution during impact and fatigue tests. On aircraft wing box sections, sensor data correlated well with numerical simulations, confirming accurate strain monitoring. The sensors also detected impacts on carbon fiber panels, suggesting potential for wide-area coverage with fewer sensors. Overall, the GNP/PDMS flexible strain sensor shows strong promise for aircraft structural health monitoring, combining high sensitivity, durability, and scalability. Future work should focus on optimizing fabrication and extending applications to broader industrial environments.

Fiberglass-reinforced composites also hold significant potential for structural health monitoring (SHM). In this context, Groo *et al*. [71] presented a detailed methodology for integrating laser-induced graphene (LIG) into fiberglass composites and evaluated their performance under fatigue loading. LIG was synthesized via a transfer-printing process in which commercial polyimide (Kapton®) films were irradiated with a CO_2 infrared laser to convert their surfaces into graphene, then embedded into uncured fiberglass prepregs under manual pressure. The laminates were cured in a hot press at 127°C and 100 psi (0.69 MPa) for 2 h, forming a robust interlayer within the composite structure. SEM analysis confirmed the successful conversion of polyimide to graphene. The LIG-embedded composites were tested under quasi-static tension and cyclic fatigue using an Instron ElectroPuls™ system, while electrical resistance was continuously monitored via a Wheatstone bridge circuit to track damage progression in real time. Digital Image Correlation (DIC) and resistance data revealed three distinct stages of fatigue damage: matrix cracking (Region I), interfacial debonding and delamination (Region II), and fiber fracture (Region III). Marked changes in electrical resistance correlated with these stages, confirming the sensor's effectiveness in identifying different damage modes. A multiphysics numerical model incorporating axial and transverse strain components was calibrated with experimental data, accurately predicting the nonlinear electromechanical response. Moreover, the first derivative of the normalized resistance provided valuable insights into fatigue life estimation, strongly correlating with failure onset. The combined use of DIC and electrical resistance measurements offered a comprehensive approach for evaluating the integrity of fiberglass composites under cyclic loading. Overall, this study demonstrated the strong potential of LIG as a reliable, real-time sensing element for life prediction and SHM of fiberglass-reinforced composites.

Graphene oxide (GO) can also be employed in laminated composites, as demonstrated by Rapisarda and Meo [72], who investigated the synthesis, characterization, and application of reduced graphene oxide (RGO) films as multifunctional coatings on carbon fiber-reinforced polymer (CFRP) laminates. The process began with the exfoliation of graphite oxide (GtO) in distilled water using probe sonication to obtain GO, which was then cast onto polyethylene terephthalate (PET) films and dried for 24 h to form GO films. These films were annealed at 1300°C for 3 h under an argon atmosphere, producing 40 µm-thick RGO films. The RGO-coated CFRP laminates were fabricated by laminating a three-ply symmetric CFRP prepreg with the RGO film on top, followed by autoclave curing at 180°C and 100 psi (0.69 MPa) for 3 h. Electrical conductivity, measured via a four-point probe, showed a substantial increase in the RGO-coated laminates compared to the reference CFRP. Wettability tests revealed that the RGO layer imparted hydrophobicity to the surface, with a contact angle of 95° versus 60° for the uncoated side. Mechanical characterization through three-point bending tests indicated a reduction in flexural modulus for the coated samples, although the RGO film exhibited strong

adhesion, detaching only after CFRP failure. During bending tests, in situ resistance monitoring showed a linear relationship between normalized resistance change and flexural strain above a threshold strain, confirming the strain-sensing capability of the RGO film due to deformation-induced changes in its conductive network. Overall, this study underscored the potential of RGO films as multifunctional coatings for CFRP laminates, offering enhanced electrical conductivity, hydrophobicity, and strain-sensing functionality while maintaining satisfactory mechanical integrity. Future research aims to deepen the understanding of RGO's influence on composite mechanical behavior and to explore DC-biased thermography for damage localization.

To elucidate recent advances and the relative performance of carbon-based sensors for structural health monitoring, a comparative analysis of CNT-, CNTY-, and graphene-based sensors was conducted. Table 1 summarizes key parameters reported in the literature, including gauge factor, sensitivity, and operating range, as well as representative applications of each material system. This comparison highlights the specific advantages and limitations of each carbon-based approach for SHM applications in composite structures.

Table 1. Comparison of key parameters for CNT-, CNTY-, and graphene-based SHM sensors.

Material	Gauge factor (GF)	Sensitivity	Operating range	Typical application	Reference
CNT	2-10	High	up to 3% strain	Composite laminates, textiles	[29–32]
CNTY	0.2-0.5	Moderate	up to 5% strain	Laminated composites	[45,49–52]
Graphene	up to 26	Very high	up to 10% strain	Thin films, GFRO, CFRP	[67–72]

The data summarized in Table 1 indicate that while CNT-based sensors exhibit excellent sensitivity and mechanical robustness, CNTY sensors provide higher structural compatibility and reliability under cyclic loading. Graphene-based sensors, on the other hand, combine superior sensitivity with wide operational strain ranges, making them particularly promising for multifunctional and non-intrusive SHM applications. Together, these results demonstrate that each carbon nanomaterial offers unique advantages depending on the desired balance between sensitivity, mechanical integration, and application environment.

3. Conclusions and Future Perspectives

Carbon-based nanomaterials, including CNTs, CNTYs, and graphene, have demonstrated remarkable potential as sensing elements for SHM in composite materials. Their superior electrical conductivity, flexibility, and mechanical performance enable accurate, real-time strain and damage detection while maintaining the structural integrity of the host material.

Recent studies have shown significant progress in developing multifunctional composites that integrate mechanical strength with sensing capabilities. CNT-based sensors offer a balance between conductivity and mechanical robustness, CNTYs provide improved structural integration and cyclic durability, and graphene sensors stand out for their high sensitivity and adaptability to flexible substrates.

Current limitations, however, include challenges related to nanomaterial dispersion, interfacial bonding, signal stability under varying environmental conditions, and the scalability of fabrication techniques. Future directions should therefore focus on developing standardized processing routes, advancing data interpretation through artificial intelligence, and integrating energy-harvesting elements into autonomous SHM systems. In terms of application readiness,

CNTY- and graphene-based sensors already exhibit promising performance in laboratory and small-scale field studies, indicating their strong potential for industrial deployment.

3.1. Challenges and future prospects.

Despite the rapid progress achieved in recent years, several key challenges remain to be overcome to ensure large-scale, long-term adoption of carbon-based SHM technologies. Uniform nanomaterial dispersion within polymer matrices remains difficult to achieve without compromising mechanical performance, and ensuring durable interfacial adhesion is critical for signal repeatability. Environmental factors, including temperature, humidity, and fatigue loading, can introduce noise and drift, requiring improved material design and signal-conditioning strategies.

Future research should emphasize scalable fabrication and sensor integration methods compatible with existing composite manufacturing processes. The incorporation of data-driven modeling and machine learning for damage prediction, as well as the development of multifunctional CNTY or graphene structures capable of energy storage and self-sensing, will enable the next generation of autonomous SHM systems. By addressing these challenges, carbon-based nanomaterial sensors will continue to advance toward reliable, intelligent, and field-ready solutions for aerospace, civil, and energy infrastructures.

Author Contributions

Conceptualization, T.L.A.M., E.A.N.S., and I.G.G.; validation, T.L.A.M., A.H.K., J.L.A., and D.A.R.; resources, D.A.R.; writing—original draft preparation, T.L.A.M., E.A.N.S., and I.G.G.; writing—review and editing, T.L.A.M., E.A.N.S., I.G.G., A.H.K., J.L.A., and D.A.R.; visualization, T.L.A.M.; supervision, D.A.R.; project administration, D.A.R.; funding acquisition, D.A.R. All authors have read and agreed to the published version of the manuscript.

Institutional Review Board Statement

Not applicable.

Informed Consent Statement

Not applicable.

Data Availability Statement

No new data were created or analyzed in this study. Data sharing is not applicable.

Funding

The authors declare that a grant from Petrobras entitled: “Desenvolvimento de sistema de monitoramento de reparos constituídos de materiais compósitos empregando fibras de nanotubos de carbono”, Contrato N° 5850.0109507.18.9, Nº SAP 4600667421, was received during the preparation of this manuscript. D. A. Rade acknowledges Conselho Nacional de Desenvolvimento Ci-entífico e Tecnológico - CNPq (grant#312068/2020-4) and Fundação de Amparo à Pesquisa do Estado de São Paulo - FAPESP (grant #2021/11258-5, project FLYMOV) for the financial support to his research work.

Acknowledgments

Declared none.

Conflicts of Interest

The authors declare no conflict of interest.

Abbreviations

The following abbreviations are used in this manuscript:

Abbreviation	Definition
AE	Acoustic Emission
AFSA	Artificial Fish Swarm Algorithm
CFRP	Carbon Fiber Reinforced Polymer
CNT / CNTs	Carbon Nanotube / Nanotubes
CNTY / CNTYs	Carbon Nanotube Yarn / Yarns
CVD	Chemical Vapor Deposition
DIC	Digital Image Correlation
EMI	Electromagnetic Interference
FBG	Fiber Bragg Grating
GF	Gauge Factor
GFRP	Glass Fiber Reinforced Polymer
GNP	Graphene Nanoplatelet
GO	Graphene Oxide
ITS	Indirect Tensile Strength
LIG	Laser-Induced Graphene
MWCNT	Multi-Walled Carbon Nanotube
NDI	Non-Destructive Inspection
NDT	Non-Destructive Testing
PAI	Polyamide-Imide
PDMS	Polydimethylsiloxane
PZT	Lead Zirconate Titanate
rGO	Reduced Graphene Oxide
SEM	Scanning Electron Microscopy
SHM	Structural Health Monitoring
SMA	Stone Mastic Asphalt
SWCNT	Single-Walled Carbon Nanotube
TEM	Transmission Electron Microscopy
UV-Vis	Ultraviolet–Visible Spectroscopy

References

1. Harussani, M.M.; Sapuan, S.M.; Nadeem, G.; Rafin, T.; Kirubaanand, W. Recent Applications of Carbon-Based Composites in Defence Industry: A Review. *Def. Technol.* **2022**, *18*, 1281–1300, https://doi.org/10.1016/j.dt.2022.03.006.
2. Hu, S.; Wang, D.; Večerník, J.; Křemenáková, D.; Militký, J. Electromagnetic Interference (EMI) Shielding and Thermal Management of Sandwich-Structured Carbon Fiber-Reinforced Composite (CFRC) for Electric Vehicle Battery Casings. *Polymers* **2024**, *16*, 2291, https://doi.org/10.3390/polym16162291.
3. Ramesh, M.; Manickam, T.S.; Arockiasamy, F.S.; Ponnusamy, B.; Sivakumar, R.; Sivakumar, P.; Kandasamy, P. Powering the future: a comprehensive review of polymer composite energy storage applications. *Eng. Proc.* **2024**, *61*, 24, https://doi.org/10.3390/engproc2024061024.
4. Razaq, A.; Bibi, F.; Zheng, X.; Papadakis, R.; Jafri, S.H.M.; Li, H. Review on Graphene-, Graphene Oxide-, Reduced Graphene Oxide-Based Flexible Composites: From Fabrication to Applications. *Materials* **2022**, *15*, 1012, https://doi.org/10.3390/ma15031012.
5. Achenbach, J.D. Structural Health Monitoring - What Is the Prescription? *Mech. Res. Commun.* **2009**, *36*, 137–142, https://doi.org/10.1016/j.mechrescom.2008.08.011.

6. Lemartinel, A.; Castro, M.; Fouché, O.; De-Luca, J.C.; Feller, J.F. A Review of Nanocarbon-Based Solutions for the Structural Health Monitoring of Composite Parts Used in Renewable Energies. *J. Compos. Sci.* **2022**, *6*, 32, https://doi.org/10.3390/jcs6020032.
7. Zhang, L.; Wang, X.; Lu, S.; Jiang, X.; Ma, C.; Lin, L.; Wang, X. Fatigue Damage Monitoring of Repaired Composite Wind Turbine Blades Using High-Stability Buckypaper Sensors. *Compos. Sci. Technol.* **2022**, *227*, 109592, https://doi.org/10.1016/j.compscitech.2022.109592.
8. Bandyopadhyay, S.; Srinivasan, A. Polymer Nanocomposites: From Synthesis to Applications. In Nanocomposites and Polymers with Analytical Methods, Cuppoletti, J., Ed.; IntechOpen: London, **2011**; https://doi.org/10.5772/17039.
9. Stobinski, L.; Lesiak, B.; Kövér, L.; Tóth, J.; Biniak, S.; Trykowski, G.; Judek, J. Multiwall Carbon Nanotubes Purification and Oxidation by Nitric Acid Studied by the FTIR and Electron Spectroscopy Methods. *J. Alloys Compd.* **2010**, *501*, 77–84, https://doi.org/10.1016/j.jallcom.2010.04.032.
10. Ajayan, P.M. Nanotubes from Carbon. *Chem. Rev.* **1999**, *99*, 1787–1800, https://doi.org/10.1021/cr970102g.
11. Dresselhaus, M.S.; Dresselhaus, G.; Saito, R.; Jorio, A. Raman Spectroscopy of Carbon Nanotubes. *Phys. Rep.* **2005**, *409*, 47–99, https://doi.org/10.1016/j.physrep.2004.10.006.
12. Coleman, J.N.; Khan, U.; Blau, W.J.; Gun'ko, Y.K. Small but Strong: A Review of the Mechanical Properties of Carbon Nanotube–Polymer Composites. *Carbon* **2006**, *44*, 1624–1652, https://doi.org/10.1016/j.carbon.2006.02.038.
13. Han, Z.; Fina, A. Thermal Conductivity of Carbon Nanotubes and Their Polymer Nanocomposites: A Review. *Prog. Polym. Sci.* **2011**, *36*, 914–944, https://doi.org/10.1016/j.progpolymsci.2010.11.004.
14. Moniruzzaman, M.; Winey, K.I. Polymer Nanocomposites Containing Carbon Nanotubes. *Macromolecules* **2006**, *39*, 5194–5205, https://doi.org/10.1021/ma060733p.
15. Ma, P.-C.; Siddiqui, N.A.; Marom, G.; Kim, J.-K. Dispersion and Functionalization of Carbon Nanotubes for Polymer-Based Nanocomposites: A Review. *Compos. Part A Appl. Sci. Manuf.* **2010**, *41*, 1345–1367, https://doi.org/10.1016/j.compositesa.2010.07.003.
16. Reddy, M.M.; Vivekanandhan, S.; Misra, M.; Bhatia, S.K.; Mohanty, A.K. Biobased Plastics and Bionanocomposites: Current Status and Future Opportunities. *Prog. Polym. Sci.* **2013**, *38*, 1653–1689, https://doi.org/10.1016/j.progpolymsci.2013.05.006.
17. Shoukat, R.; Khan, M.I. Carbon Nanotubes: A Review on Properties, Synthesis Methods and Applications in Micro and Nanotechnology. *Microsyst. Technol.* **2021**, *27*, 4183–4192, https://doi.org/10.1007/s00542-021-05211-6.
18. Luo, M.; Li, Y.; Jin, S.; Sang, S.; Zhao, L.; Wang, Q.; Li, Y. Microstructure and Mechanical Properties of Multi-Walled Carbon Nanotubes Containing Al2O3–C Refractories with Addition of Polycarbosilane. *Ceram. Int.* **2013**, *39*, 4831–4838, https://doi.org/10.1016/j.ceramint.2012.11.075.
19. Khaniki, H.B.; Ghayesh, M.H. A Review on the Mechanics of Carbon Nanotube Strengthened Deformable Structures. *Eng. Struct.* **2020**, *220*, 110711, https://doi.org/10.1016/j.engstruct.2020.110711.
20. de Souza Vieira, L.; dos Anjos, E.G.R.; Verginio, G.E.A.; Oyama, I.C.; Braga, N.F.; da Silva, T.F.; Montagna, L.S.; Rezende, M.C.; Passador, F.R. Carbon-Based Materials as Antistatic Agents for the Production of Antistatic Packaging: A Review. *J. Mater. Sci. Mater. Electron.* **2021**, *32*, 3929–3947, https://doi.org/10.1007/s10854-020-05178-6.
21. Montanheiro, T.L.A.; Montagna, L.S.; Machado, J.P.B.; Lemes, A.P. Covalent Functionalization of MWCNT with PHBV Chains: Evaluation of the Functionalization and Production of Nanocomposites. *Polym. Compos.* **2019**, *40*, 288–295, https://doi.org/10.1002/pc.24644.
22. Rathinavel, S.; Priyadharshini, K.; Panda, D. A Review on Carbon Nanotube: An Overview of Synthesis, Properties, Functionalization, Characterization, and the Application. *Mater. Sci. Eng. B* **2021**, *268*, 115095, https://doi.org/10.1016/j.mseb.2021.115095.
23. Baughman, R.H.; Zakhidov, A.A.; de Heer, W.A. Carbon Nanotubes--the Route Toward Applications. *Science* **2002**, *297*, 787–792, https://doi.org/10.1126/science.1060928.
24. 1. Jian, M.Q.; Xie, H.H.; Xia, K.L.; Zhang, Y.Y. Chapter 15 - Challenge and Opportunities of Carbon Nanotubes. In Industrial Applications of Carbon Nanotubes; Peng, H., Li, Q., Chen, T., Eds.; Elsevier: Boston, **2017**; pp. 433-476, https://doi.org/10.1016/B978-0-323-41481-4.00015-0.
25. Menezes, B.R.C. de; Rodrigues, K.F.; Fonseca, B.C. da S.; Ribas, R.G.; Montanheiro, T.L. do A.; Thim, G.P. Recent Advances in the Use of Carbon Nanotubes as Smart Biomaterials. *J. Mater. Chem. B* **2019**, *7*, 1343–1360, https://doi.org/10.1039/C8TB02419G.

26. Narang, A.S.; Mahato, R.I. Organ Specific Drug Delivery and Targeting to the Lungs, 1st Edition; CRC Press: Boca Raton, **2022**; https://doi.org/10.1201/9781003182566.
27. Haghgoo, M.; Hassanzadeh-Aghdam, M.K.; Ansari, R. A Comprehensive Evaluation of Piezoresistive Response and Percolation Behavior of Multiscale Polymer-Based Nanocomposites. *Compos. Part A Appl. Sci. Manuf.* **2020**, *130*, 105735, https://doi.org/10.1016/j.compositesa.2019.105735.
28. Dresselhaus, M.S.; Jorio, A.; Hofmann, M.; Dresselhaus, G. Perspectives on Carbon Nanotubes and Graphene Raman Spectroscopy. *Nano Lett.* **2010**, *10*, 751–758, https://doi.org/10.1021/nl904286r.
29. Al-Bahrani, M.; Cree, A. Micro-Scale Damage Sensing in Self-Sensing Nanocomposite Material Based CNTs. *Compos. Part B Eng.* **2021**, *205*, 108479, https://doi.org/10.1016/j.compositesb.2020.108479.
30. Duan, Q.; Lan, B.; Lv, Y. Highly Dispersed, Adhesive Carbon Nanotube Ink for Strain and Pressure Sensors. *ACS Appl. Mater. Interfaces* **2022**, *14*, 1973–1982, https://doi.org/10.1021/acsami.1c20133.
31. Chen, X.; Cheng, S.; Wang, S.; Wen, K.; Shi, C.; Zhang, J.; Zhao, D.; Han, Y.; Chen, X.; Li, B. Embedding stretchable, mesh-structured piezoresistive sensor for in-situ damage detection of glass fiber-reinforced composite. *Compos. Sci. Technol.* **2023**, *233*, 109926, https://doi.org/10.1016/j.compscitech.2023.109926.
32. Wang, M.; Li, N.; Wang, G.D.; Lu, S.W.; Zhao, Q. Di; Liu, X.L. High-Sensitive Flexural Sensors for Health Monitoring of Composite Materials Using Embedded Carbon Nanotube (CNT) Buckypaper. *Compos. Struct.* **2021**, *261*, 113280, https://doi.org/10.1016/j.compstruct.2020.113280.
33. Jiang, K.; Li, Q.; Fan, S. Spinning Continuous Carbon Nanotube Yarns. *Nature* **2002**, *419*, 801, https://doi.org/10.1038/419801a.
34. Liu, K.; Sun, Y.; Zhou, R.; Zhu, H.; Wang, J.; Liu, L.; Fan, S.; Jiang, K. Carbon Nanotube Yarns with High Tensile Strength Made by a Twisting and Shrinking Method. *Nanotechnology* **2010**, *21*, 045708, https://doi.org/10.1088/0957-4484/21/4/045708.
35. Jorio, A.; Dresselhaus, G.; Dresselhaus, M.S. Carbon Nanotubes: Advanced Topics in the Synthesis, Structure, Properties and Applications; Springer Berlin Heidelberg: Berlin, Heidelberg, **2008**; https://doi.org/10.1007/978-3-540-72865-8.
36. Dalton, A.B.; Collins, S.; Muñoz, E.; Razal, J.M.; Ebron, V.H.; Ferraris, J.P.; Coleman, J.N.; Kim, B.G.; Baughman, R.H. Super-Tough Carbon-Nanotube Fibres. *Nature* **2003**, *423*, 703–703, https://doi.org/10.1038/423703a.
37. Zhang, M.; Atkinson, K.R.; Baughman, R.H. Multifunctional Carbon Nanotube Yarns by Downsizing an Ancient Technology. *Science* **2004**, *306*, 1358–1361, https://doi.org/10.1126/science.1104276.
38. Gong, F.; Duong, H.M.; Liu, P.; Tran, T.Q. Advanced Fabrication and Properties of Aligned Carbon Nanotube Composites: Experiments and Modeling. In Carbon Nanotubes - Current Progress of their Polymer Composites, Berber, M.R., Hafez, I.H., Eds.; IntechOpen: London, **2016**; https://doi.org/10.5772/62510.
39. Li, Y.-L.; Kinloch, I.A.; Windle, A.H. Direct Spinning of Carbon Nanotube Fibers from Chemical Vapor Deposition Synthesis. *Science* **2004**, *304*, 276–278, https://doi.org/10.1126/science.1094982.
40. Behabtu, N.; Young, C.C.; Tsentalovich, D.E.; Kleinerman, O.; Wang, X.; Ma, A.W.K.; Bengio, E.A.; ter Waarbeek, R.F.; de Jong, J.J.; Hoogerwerf, R.E.; Fairchild, S.B.; Ferguson, J.B.; Maruyama, B.; Kono, J.; Talmon, Y.; Cohen, Y.; Otto, M.J.; Pasquali, M. Strong, Light, Multifunctional Fibers of Carbon Nanotubes with Ultrahigh Conductivity. *Science* **2013**, *339*, 182–186, https://doi.org/10.1126/science.1228061.
41. Choi, E.S.; Brooks, J.S.; Eaton, D.L.; Al-Haik, M.S.; Hussaini, M.Y.; Garmestani, H.; Li, D.; Dahmen, K. Enhancement of Thermal and Electrical Properties of Carbon Nanotube Polymer Composites by Magnetic Field Processing. *J. Appl. Phys.* **2003**, *94*, 6034–6039, https://doi.org/10.1063/1.1616638.
42. Zhang, C.; Song, Y.; Zhang, H.; Lv, B.; Qiao, J.; Yu, N.; Zhang, Y.; Di, J.; Li, Q. Mechanical Properties of Carbon Nanotube Fibers at Extreme Temperatures. *Nanoscale* **2019**, *11*, 4585–4590, https://doi.org/10.1039/C8NR09637F.
43. Jayasinghe, C.; Chakrabarti, S.; Schulz, M.J.; Shanov, V. Spinning Yarn from Long Carbon Nanotube Arrays. *J. Mater. Res.* **2011**, *26*, 645–651, https://doi.org/10.1557/jmr.2010.91.
44. Schulz, M.J.; Kim, S.Y.; Kubley, A.; Mast, D.; Shanov, V. Nanotube Sheet and Yarn Manufacturing and Commercialization. *WSEAS Trans. Bus. Econ.* **2021**, *18*, 1149–1163, https://doi.org/10.37394/23207.2021.18.108.
45. Vigolo, B.; Pénicaud, A.; Coulon, C.; Sauder, C.; Pailler, R.; Journet, C.; Bernier, P.; Poulin, P. Macroscopic Fibers and Ribbons of Oriented Carbon Nanotubes. *Science* **2000**, *290*, 1331–1334, https://doi.org/10.1126/science.290.5495.1331.
46. Kumar, M.; Ando, Y. Chemical Vapor Deposition of Carbon Nanotubes: A Review on Growth Mechanism

and Mass Production. *J. Nanosci. Nanotechnol.* **2010**, *10*, 3739–3758, https://doi.org/10.1166/jnn.2010.2939.
47. Zhang, X.; Li, Q.; Tu, Y.; Li, Y.; Coulter, J.Y.; Zheng, L.; Zhao, Y.; Jia, Q.; Peterson, D.E.; Zhu, Y. Strong Carbon-Nanotube Fibers Spun from Long Carbon-Nanotube Arrays. *Small* **2007**, *3*, 244–248, https://doi.org/10.1002/smll.200600368.
48. Thostenson, E.T.; Ren, Z.; Chou, T.-W. Advances in the Science and Technology of Carbon Nanotubes and Their Composites: A Review. *Compos. Sci. Technol.* **2001**, *61*, 1899–1912, https://doi.org/10.1016/S0266-3538(01)00094-X.
49. Abot, J.L.; Montanheiro, T.L.A.; Pereira, D. de A.; Nascimento, S.; Nascimento, C.L.; Silva, J.R.B.F.; Kasama, A.H.; Rade, D.A. Monitoring of Static and Vibration Responses of Laminated Composite Materials Using Integrated Carbon Nanotube Fibers. *Compos. Sci. Technol.* **2024**, *254*, 110694, https://doi.org/10.1016/j.compscitech.2024.110694.
50. Wang, H.; Jia, Y.; Jia, M.; Pei, X.; Wan, Z. Damage Monitoring of Braided Composites Using CNT Yarn Sensor Based on Artificial Fish Swarm Algorithm. *Sensors* **2023**, *23*, 7067, https://doi.org/10.3390/s23167067.
51. Binfaris, A.S.; Zestos, A.G.; Abot, J.L. Development of Carbon Nanotube Yarn Supercapacitors and Energy Storage for Integrated Structural Health Monitoring. *Energies* **2023**, *16*, 5736, https://doi.org/10.3390/en16155736.
52. Uribe-Riestra, G.; Pech-Pisté, R.; Avilés, F. Integration of Carbon Nanotube Yarns into Glass-fiber Reinforced Composites for Electrical Self-sensing of Damage under Cyclic Bending and Impact Loading. *Polym. Compos.* **2024**, *45*, 15547-15560, https://doi.org/10.1002/pc.28849.
53. Geim, A.K.; Novoselov, K.S. The Rise of Graphene. *Nat. Mater.* **2007**, *6*, 183–191, https://doi.org/10.1038/nmat1849.
54. Ferrari, A.C. Raman Spectroscopy of Graphene and Graphite: Disorder, Electron-Phonon Coupling, Doping and Nonadiabatic Effects. *Solid State Commun.* **2007**, *143*, 47–57, https://doi.org/10.1016/j.ssc.2007.03.052.
55. Chatterjee, S.; Wang, J.W.; Kuo, W.S.; Tai, N.H.; Salzmann, C.; Li, W.L.; Hollertz, R.; Nüesch, F.A.; Chu, B.T.T. Mechanical Reinforcement and Thermal Conductivity in Expanded Graphene Nanoplatelets Reinforced Epoxy Composites. *Chem. Phys. Lett.* **2012**, *531*, 6–10, https://doi.org/10.1016/j.cplett.2012.02.006.
56. Khine, Y.Y.; Wen, X.; Jin, X.; Foller, T.; Joshi, R. Functional Groups in Graphene Oxide. *Phys. Chem. Chem. Phys.* **2022**, *24*, 26337–26355, https://doi.org/10.1039/D2CP04082D.
57. Wu, Y.; Wang, Y.; Wang, S.; Fan, X.; Liu, Y.; Zhao, R.; Hou, H.; Zha, Y.; Zou, J. The Combination of Graphene Oxide and Preservatives Can Further Improve the Preservation of Cut Flowers. *Front. Plant Sci.* **2023**, *14*, https://doi.org/10.3389/fpls.2023.1121436.
58. Wu, S.; Qureshi, T.; Wang, G. Application of Graphene in Fiber-Reinforced Cementitious Composites: A Review. *Energies* **2021**, *14*, 4614, https://doi.org/10.3390/en14154614.
59. Urade, A.R.; Lahiri, I.; Suresh, K.S. Graphene Properties, Synthesis and Applications: A Review. *JOM* **2023**, *75*, 614–630, https://doi.org/10.1007/s11837-022-05505-8.
60. Heyl, M.; List-Kratochvil, E.J.W. Only Gold Can Pull This off: Mechanical Exfoliations of Transition Metal Dichalcogenides beyond Scotch Tape. *Appl. Phys. A* **2023**, *129*, 16, https://doi.org/10.1007/s00339-022-06297-z.
61. Salverda, M.; Thiruppathi, A.R.; Pakravan, F.; Wood, P.C.; Chen, A. Electrochemical Exfoliation of Graphite to Graphene-Based Nanomaterials. *Molecules* **2022**, *27*, 8643, https://doi.org/10.3390/molecules27248643.
62. Saeed, M.; Alshammari, Y.; Majeed, S.A.; Al-Nasrallah, E. Chemical Vapour Deposition of Graphene—Synthesis, Characterisation, and Applications: A Review. *Molecules* **2020**, *25*, 3856, https://doi.org/10.3390/molecules25173856.
63. Moreno-Bárcenas, A.; Perez-Robles, J.F.; Vorobiev, Y. V.; Ornelas-Soto, N.; Mexicano, A.; García, A.G. Graphene Synthesis Using a CVD Reactor and a Discontinuous Feed of Gas Precursor at Atmospheric Pressure. *J. Nanomater.* **2018**, *2018*, 3457263, https://doi.org/10.1155/2018/3457263.
64. Zubair, M.; Farooq, S.; Hussain, A.; Riaz, S.; Ullah, A. A Review of Current Developments in Graphene Oxide–Polysulfone Derived Membranes for Water Remediation. *Environ. Sci. Adv.* **2024**, *3*, 983–1003, https://doi.org/10.1039/D4VA00058G.
65. Khan, M.; Al-Marri, A.H.; Khan, M.; Shaik, M.R.; Mohri, N.; Adil, S.F.; Kuniyil, M.; Alkhathlan, H.Z.;

Al-Warthan, A.; Tremel, W.; Tahir, M.N.; Siddiqui, M.R.H. Green Approach for the Effective Reduction of Graphene Oxide Using Salvadora Persica L. Root (Miswak) Extract. *Nanoscale Res. Lett.* **2015**, *10*, 281, https://doi.org/10.1186/s11671-015-0987-z.

66. Thiyagarajulu, N.; Arumugam, S. Green Synthesis of Reduced Graphene Oxide Nanosheets Using Leaf Extract of Lantana Camara and Its In-Vitro Biological Activities. *J. Clust. Sci.* **2021**, *32*, 559–568, https://doi.org/10.1007/s10876-020-01814-7.
67. Wang, Q.; Tian, Y.; Duongthipthewa, A.; Zhang, J.; Liu, M.; Su, Z.; Zhou, L. An Embedded Non-Intrusive Graphene/Epoxy Broadband Nanocomposite Sensor Co-Cured with GFRP for in Situ Structural Health Monitoring. *Compos. Sci. Technol.* **2023**, *236*, 109995, https://doi.org/10.1016/j.compscitech.2023.109995.
68. Guan, R.; Zou, F.; Li, D.; Yao, Y. A High-Thermal-Stability, Fully Spray Coated Multilayer Thin-Film Graphene/Polyamide-Imide Nanocomposite Strain Sensor for Acquiring High-Frequency Ultrasonic Waves. *Compos. Sci. Technol.* **2022**, *227*, 109628, https://doi.org/10.1016/j.compscitech.2022.109628.
69. Gulisano, F.; Abedi, M.; Jurado-Piña, R.; Apaza, F.R.A.; Roshan, M.J.; Fangueiro, R.; Correia, A.G.; Gallego, J. Stress and Damage-Sensing Capabilities of Asphalt Mixtures Incorporating Graphene Nanoplatelets. *Sensors Actuators A Phys.* **2023**, *359*, 114494, https://doi.org/10.1016/j.sna.2023.114494.
70. Meng, Q.; Zhao, J.; Zhou, Z.; Han, S.; Feng, Y.; Han, Q.; Liu, T. Damage Monitoring of Aircraft Structural Components Based on Large-Area Flexible Graphene Strain Sensors. *Sensors Actuators A Phys.* **2024**, *369*, 115092, https://doi.org/10.1016/j.sna.2024.115092.
71. Groo, L.A.; Nasser, J.; Inman, D.; Sodano, H. Fatigue Damage Tracking and Life Prediction of Fiberglass Composites Using a Laser Induced Graphene Interlayer. *Compos. Part B Eng.* **2021**, *218*, 108935, https://doi.org/10.1016/j.compositesb.2021.108935.
72. Rapisarda, M.; Meo, M. Multifunctional Reduced Graphene Oxide Coating on Laminated Composites. *Mater. Today Proc.* **2021**, *34*, 149–155, https://doi.org/10.1016/j.matpr.2020.01.612.

Publisher's Note & Disclaimer